

Preparation of new inorganic–organic complexes by using $\text{Fe}_x\text{Ti}_{1-2x}\text{Nb}_{1+x}\text{O}_5^-$ ($x = 0-0.5$) nanosheets

G. K. Prasad · M. Horiuchi · N. Kumada · Y. Yonesaki · T. Takei · N. Kinomura

Received: 7 July 2006 / Accepted: 2 August 2007 / Published online: 22 September 2007
© Springer Science+Business Media, LLC 2007

Abstract Novel inorganic–organic complex nanocomposites have been prepared by using exfoliated $\text{Fe}_x\text{Ti}_{1-2x}\text{Nb}_{1+x}\text{O}_5^-$ nanosheets and poly (*N*-octadecyl-2-ethynyl pyridinium bromide) (PNOEtPyBr) by the method of exfoliation–reflocculation. The X-ray diffraction data of the nanocomposites indicate the formation of $\text{Fe}_x\text{Ti}_{1-2x}\text{Nb}_{1+x}\text{O}_5^-/\text{PNOEtPyBr}$ nanostructure with the length of basal spacing of 4.6 nm along the stacking direction of $\text{Fe}_x\text{Ti}_{1-2x}\text{Nb}_{1+x}\text{O}_5^-$ nanosheet layers. The a. c. electrical conductivity of nanocomposites decreased with the value of x . This trend was correlated with the hydration behavior of the interlayer for $\text{HFe}_x\text{Ti}_{1-2x}\text{Nb}_{1+x}\text{O}_5 \cdot n\text{H}_2\text{O}$ ($x = 0-0.5$) which were starting compounds of nanosheets.

Introduction

Hybrid inorganic–organic nanocomposites based on conducting polymers and exfoliated unilamellar nanosheet crystallites have been attracting tremendous interest due to their potential application in various devices, such as photovoltaic cells, sensors, and capacitors [1–3]. In these nanocomposites, host and guest components are interleaved, while lamellar nature and the properties of the host material are inherited in the product phase, although the guest species cause the expansion of interlayer spacing. Recently, we have prepared nanocomposites based on

$\text{Mg}_{0.04}\text{Nb}_{1.66}\text{O}_5^-$ [4], NbWO_6^- [5] and SbP_2O_8^- [6] nanosheets and ionic polyacetylene. The nanocomposite of $\text{Mg}_{0.04}\text{Nb}_{1.66}\text{O}_5^-$ exhibited unique a. c. conductivity and dielectric property. Inspired by this, we have attempted to prepare the nanocomposite based on $\text{Fe}_x\text{Ti}_{1-2x}\text{Nb}_{1+x}\text{O}_5^-$ nanosheets and the ionic polyacetylene. $\text{Fe}_x\text{Ti}_{1-2x}\text{Nb}_{1+x}\text{O}_5^-$ nanosheets were prepared from $\text{HFe}_x\text{Ti}_{1-2x}\text{Nb}_{1+x}\text{O}_5 \cdot n\text{H}_2\text{O}$ ($x = 0-0.5$) [7] whose crystal structure is the same as that of the starting compound ($\text{HMg}_{0.34}\text{Nb}_{1.66}\text{O}_5 \cdot n\text{H}_2\text{O}$) of $\text{Mg}_{0.04}\text{Nb}_{1.66}\text{O}_5^-$ nanosheets. The series of $\text{HFe}_x\text{Ti}_{1-2x}\text{Nb}_{1+x}\text{O}_5 \cdot n\text{H}_2\text{O}$ exhibited unique hydration behavior of the interlayer; easiness of hydration increased with the value of x and no hydration was observed for $x = 0$ and 0.125, and the interlayer of $\text{HMg}_{0.34}\text{Nb}_{1.66}\text{O}_5 \cdot n\text{H}_2\text{O}$ was hydrated easily in air like $\text{HFe}_{0.5}\text{Nb}_{1.5}\text{O}_5 \cdot n\text{H}_2\text{O}$ [7]. We have investigated the relation between this hydration trend and nature of nanocomposite with the ionic polyacetylene.

Experimental

Series of protonated layer compounds, $\text{HFe}_x\text{Ti}_{1-2x}\text{Nb}_{1+x}\text{O}_5 \cdot n\text{H}_2\text{O}$ were prepared based on previously published method [7]. $\text{Fe}_x\text{Ti}_{1-2x}\text{Nb}_{1+x}\text{O}_5^-$ nanosheet dispersions were obtained by exfoliation of $\text{HFe}_x\text{Ti}_{1-2x}\text{Nb}_{1+x}\text{O}_5 \cdot n\text{H}_2\text{O}$ using tetra butyl ammonium hydroxide (TBAOH) solution. Exfoliation was achieved by stirring 1.0 g of $\text{HFe}_x\text{Ti}_{1-2x}\text{Nb}_{1+x}\text{O}_5 \cdot n\text{H}_2\text{O}$ in a 250 mL of TBAOH solution for a week. The molar ratio of TBAOH and $\text{HFe}_x\text{Ti}_{1-2x}\text{Nb}_{1+x}\text{O}_5 \cdot n\text{H}_2\text{O}$ was 0.5. Unexfoliated $\text{HFe}_x\text{Ti}_{1-2x}\text{Nb}_{1+x}\text{O}_5 \cdot n\text{H}_2\text{O}$ was separated by filtration and then a stable dispersion solution of $\text{Fe}_x\text{Ti}_{1-2x}\text{Nb}_{1+x}\text{O}_5^-$ nanosheets was obtained. Inorganic–organic complex nanocomposites were prepared by mixing nanosheet solution (15 mL) to the alcoholic solution (10 mL) of poly (*N*-octadecyl-2-ethynyl

G. K. Prasad · M. Horiuchi · N. Kumada (✉) · Y. Yonesaki · T. Takei · N. Kinomura
Department of Research Interdisciplinary, Graduate School of Medicine and Engineering, University of Yamanashi, Miyamae-cho 7, Kofu 400-8511, Japan
e-mail: kumada@yamanashi.ac.jp

pyridinium bromide) (PNOEtPyBr) (0.02 g) under stirring conditions. After stirring for 1 h, it was centrifuged at 10,000 rpm for 20 min while washing with distilled water. Thereafter, complex was dried at 60 °C for 12 h prior to its characterization and then, polymer and nanocomposite complexes were doped with bromine by using vapor adsorption method [4]. The products were identified by X-ray powder diffraction pattern using monochromated $\text{CuK}\alpha$ radiation. The FT-IR spectra of the powder samples were measured in the range of 4,000–400 cm^{-1} with KBr pellet method. The thermal stability was investigated by TG-DTA with a heating rate of 10°/min. For the measurement of a. c. conductivity of nanocomposite complexes, the powder samples were compressed under the pressure of 15 kN and the pellets of 10 mm diameter were obtained. The a. c. conductivity was measured by using a chemical impedance meter within a frequency range from 10 Hz to 1 MHz at room temperature.

Results and discussion

The XRD patterns of $\text{Fe}_x\text{Ti}_{1-2x}\text{Nb}_{1+x}\text{O}_5/\text{PNOEtPyBr}$ complexes can be attributed to the scattering of X-rays from the $\text{Fe}_x\text{Ti}_{1-2x}\text{Nb}_{1+x}\text{O}_5$ nanosheet layers as shown in Fig. 1. They are independent of the value of x and the length (4.6 nm) of the basal spacing as well. Obtained data are compared also with that of the previously reported $\text{Mg}_{0.04}\text{Nb}_{1.66}\text{O}_5/\text{PNOEtPyBr}$ complex [4] and this suggests that the conformation of polymer molecules in $\text{Fe}_x\text{Ti}_{1-2x}\text{Nb}_{1+x}\text{O}_5/\text{PNOEtPyBr}$ complexes is same as that of $\text{Mg}_{0.04}\text{Nb}_{1.66}\text{O}_5/\text{PNOEtPyBr}$. The conformation of polymer molecules and the length of basal spacing within the

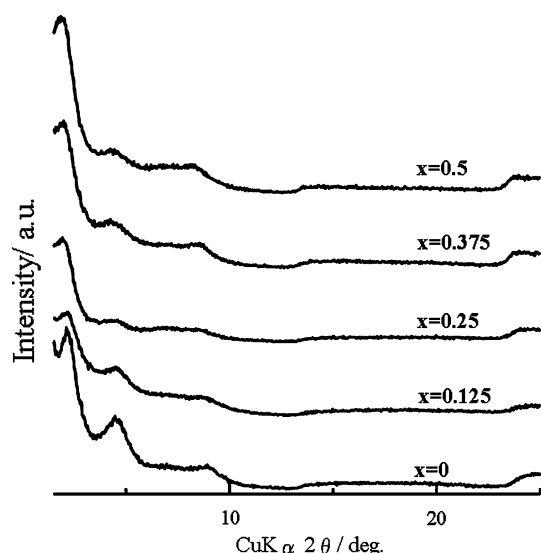


Fig. 1 XRD patterns of $\text{Fe}_x\text{Ti}_{1-2x}\text{Nb}_{1+x}\text{O}_5/\text{PNOEtPyBr}$ complexes

$\text{Fe}_x\text{Ti}_{1-2x}\text{Nb}_{1+x}\text{O}_5$ nanosheet layers are considerably dependent on the position and size of functional groups present on the guest polymer molecule [6, 8]. The *N*-octadecyl-2-ethynyl groups of the polymer molecules are oriented at an angle of 53° within the galleries of $\text{Fe}_x\text{Ti}_{1-2x}\text{Nb}_{1+x}\text{O}_5$ nanosheet layers as illustrated in Fig. 2. This value was estimated from the thickness (0.76 nm) of nanosheets and comparison of the height of PNOEtPyBr molecules (4.8 nm, bilayer) and the experimental expansion (3.84 nm). The tilted orientation is attained by the polymer molecules in order to minimize the steric repulsions within the nanostructure. The FT-IR spectra and TG curves are shown in Figs. 3 and 4. The FT-IR spectra indicate absorption assigned as follows; the conjugated structure ($-\text{C}=\text{C}-$ double bonds) at 1620 and 1500 cm^{-1} , $-\text{CH}_2-$ stretching of alkyl chain at 2,926 and 2,852 cm^{-1} . The values (43–47 mass%) of the mass loss and the TG-curves for $\text{Fe}_x\text{Ti}_{1-2x}\text{Nb}_{1+x}\text{O}_5/\text{PNOEtPyBr}$ complexes were similar to each other, and the ratio of PNOEtPyBr and $\text{Fe}_x\text{Ti}_{1-2x}\text{Nb}_{1+x}\text{O}_5$ in complexes was calculated to be 0.4–0.5 from the mass loss from 200 to 600 °C which corresponds to decomposition of polymer. Consequently the structure of $\text{Fe}_x\text{Ti}_{1-2x}\text{Nb}_{1+x}\text{O}_5/\text{PNOEtPyBr}$ complexes is independent of the hydration trend in the interlayer of $\text{HFe}_x\text{Ti}_{1-2x}\text{Nb}_{1+x}\text{O}_5 \cdot n\text{H}_2\text{O}$. The $\text{Fe}_x\text{Ti}_{1-2x}\text{Nb}_{1+x}\text{O}_5/\text{PNOEtPyBr}$ complexes exhibit the a. c. electrical conductivity in the range of $\sim 10^{-4}$ – 10^{-5} S cm^{-1} in the doped form which

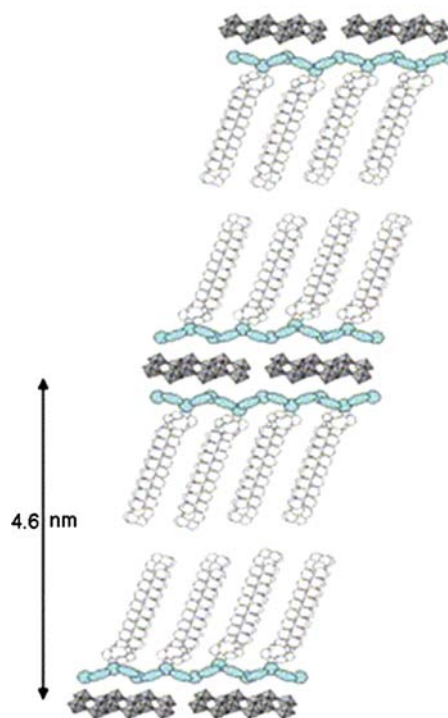


Fig. 2 Schematic representation of nanostructure for $\text{Fe}_x\text{Ti}_{1-2x}\text{Nb}_{1+x}\text{O}_5/\text{PNOEtPyBr}$ complexes

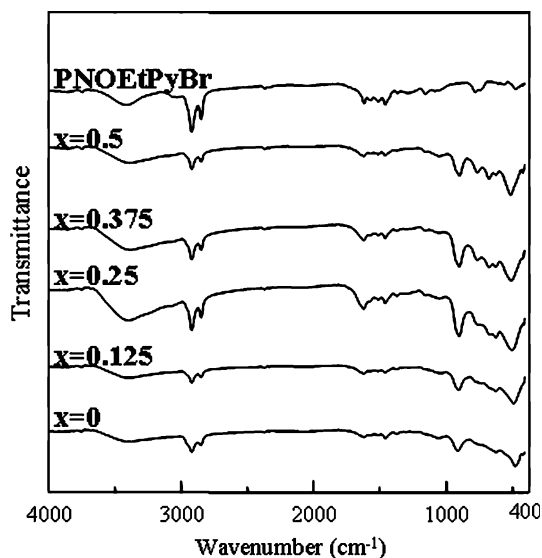


Fig. 3 FT-IR spectra of PNOEtPyBr and $\text{Fe}_x\text{Ti}_{1-2x}\text{Nb}_{1+x}\text{O}_5/\text{PNOEtPyBr}$ complexes

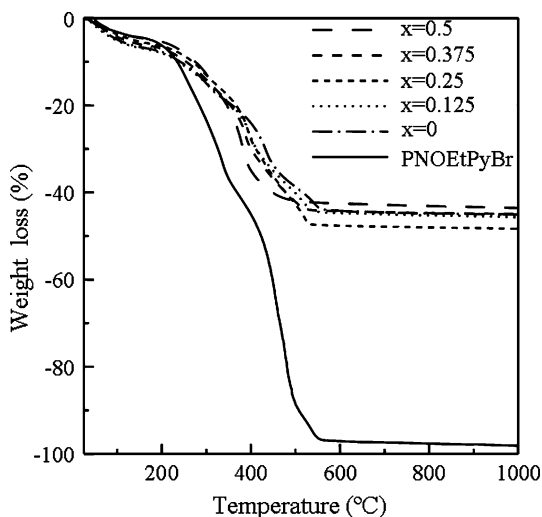


Fig. 4 TG curves of PNOEtPyBr and $\text{Fe}_x\text{Ti}_{1-2x}\text{Nb}_{1+x}\text{O}_5/\text{PNOEtPyBr}$ complexes

are lower than that of the doped polymer (PNO) ($\sim 10^{-3} \text{ S cm}^{-1}$) as illustrated in Fig. 5. This result is consistent with the previously reported data [4]. The frequency dependence of the a. c. electrical conductivity can be interpreted by the charge transport mechanisms, which are influenced by two processes, hopping and tunneling of charge carriers over the potential barrier of the formed interface. The a. c. electrical conductivity for $\text{Fe}_x\text{Ti}_{1-2x}\text{Nb}_{1+x}\text{O}_5/\text{PNOEtPyBr}$ complexes exhibits similar frequency dependence with each other and decreases with the

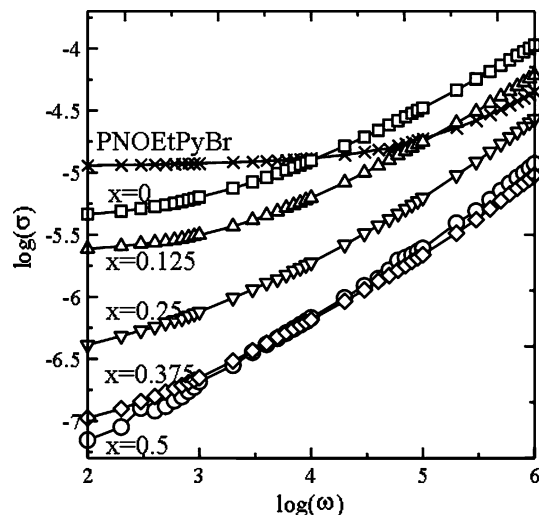


Fig. 5 Frequency dependence of a. c. conductivity of PNOEtPyBr and $\text{Fe}_x\text{Ti}_{1-2x}\text{Nb}_{1+x}\text{O}_5/\text{PNOEtPyBr}$ complexes

value of x in low frequency region. The increase of Fe content in the nanosheet makes the a. c. electrical conductivity for complexes lower. This trend corresponds to the hydration behavior in the interlayer of $\text{HFe}_x\text{Ti}_{1-2x}\text{Nb}_{1+x}\text{O}_5 \cdot n\text{H}_2\text{O}$. The easiness of hydration increases with the value of x and no hydration was observed for $x = 0$ and 0.125. The inability to hydrate was explained by the three-dimensional interlayer structure in which the adjacent layers are bound by the hydrogen bonds [9]. The ability of forming hydrogen bonding may contribute the charge transport in the polymer.

Acknowledgement This work was supported financially by Grant-in-Aid for Scientific Research (No.16350113) of JSPS (Japan Society for the Promotion of Science).

References

1. Regan BO, Gratzel M (1991) *Nature* 353:737
2. Alberti G, Carbone A, Palombari R (2002) *Sensors Actuat B: Chem* 2–3:150
3. Gomez-Romero P, Chojak M, Cuentas-Gallegos K, Asensio JA, Kulesza PJ, Casan-Pastor N, Lira-Cantu M (2003) *Electrochem Commun* 5:149
4. Prasad GK, Takei T, Yonesaki Y, Kumada N, Kinomura N (2005) *J Colloids Interf Sci* 288:200
5. Prasad GK, Takei T, Arimoto K, Yonesaki Y, Kumada N, Kinomura N (2006) *Solid State Ionics* 177(1–2):197
6. Prasad GK, Kumada N, Yamanaka J, Yonesaki Y, Takei T, Kinomura N (2006) *J Colloids Interf Sci* 297:654
7. Kumada N, Iwase E, Kinomura N (1998) *Mater Res Bull* 33:1729
8. Kinomura N, Kumada N (1992) *Solid State Ionics* 51:1
9. Rebbah H, Panneier J, Raveau B (1982) *J Solid State Chem* 41:57